12TH INTERNATIONAL SYMPOSIUM ON FLOW VISUALIZATION
September 10-14, 2006, German Aerospace Center (DLR), Göttingen, Germany

QUALITY ANALYSIS OF FLOW FIELD DATA DETERMINED BY 3D PTV IN GAS FLOWS

Torsten Putze
TU Dresden, Insitiute for Photogrammetry and Remote Sensing, Helmholtzstraße 10, 0162 Dresden, Germany

Keywords: *3D-PTV, multi image analysis, spatio temporal matching, photogrammetry*

ABSTRACT

3D Particle Tracking Velocimetry (3DPTV) is a fully 3D flow measurement technique delivering 3D velocity vectors and particle trajectories over large 3D observation volumes. The paper shows the development of a 3D PTV system for application in gas flow, with observation volumes ranging from (0.3 m)³ to (3 m)³. Adjusting the hardware components and the configuration to the measurement task and using appropriate strategies, 3D point errors less than 1 mm can be achieved in large observation volumes (up to some cubic metre). Results and achievable accuracies are shown in two experiment configurations.

1 INTRODUCTION

3D Particle Tracking Velocimetry (3D PTV) is a flexible technique for the determination of 3D velocity fields in liquid or gas. For that purpose a flow is densely visualised by particles and recorded by a multi camera system. For each epoch 3D object coordinates are determined for all tracer particles. Finally this method delivers time dependent 3D3C (3 dimensional, 3 component) vector fields analysing the 3D trajectories of the seeded tracers. One measurement period consists of either thousands of epochs or takes some seconds. The necessary hardware components to determine the 3D object coordinates of each tracer particle are easy to handle and can be adapted to several measurement tasks. Observation volumes up to some cubic metres can be realised. The analysis algorithms are independent of size or velocity. Nevertheless, there is a limiting correlation between the size of the observation volume, the size of the tracer particles, the image size, the frame rate of the used camera and the necessary illumination. To determine a fast flow in a very large volume e.g. a lot of hardware effort is necessary.

2 HARDWARE CONFIGURATIONS

In order to determine dynamic 3D object coordinates, at least two images taken synchronously are necessary. In case of a densely seeded flow, four cameras are required to solve the ambiguities of multi image matching [3] (cap 3.2). The used cameras are arranged convergent to achieve suitable intersections. As mentioned before, there are correlations between observation volume, flow velocity and camera characteristics. In [5] is shown, that a high speed camera system is essential to determine high dynamic processes (cap.2.1). Considering the synchronisation and the costs of multi high speed camera systems a mirror system is developed to generate virtual cameras and solve these problems [6]. Large observation volumes require bigger image format. In case of some cubic metres

observation volume SLR cameras (single lens reflex) are necessary to detect small tracer particles. This leads to a very low frame rate so that only slow flows (chap 2.2) can be analysed.

2.1 Experiment *A* – drawn wind tunnel

For the development of new methods of 3D PTV several experiments are arranged in a draw tunnel with a profile of 60 x 60 cm². Two boundaries are made of plexiglass as optical interface. Inside the channel different objects are placed to analyse their influence on the flow field. The illuminated observation volume covers 30 x 20 x 30 cm³ and the flow velocity is about 7 m/s. To determine the drift of the used tracer particles additional free fall experiments in a low pressure tank are carried out.
As mentioned before, a multi camera system is necessary to determine 3D object coordinates with image based methods. In our case only one high speed camera with 1 MPixel image size is available. By using a flexible four mirror system four virtual cameras with reduced active image size are generated [7]. Figure 1 shows the image parts of the four virtual cameras on one sensor. The mirror system can be modified to vary the intersection geometry and the observation volume. For the mentioned experiments the mean distance between observation volume and cameras is 1 meter. Besides the advantage of reduced hardware effort no synchronisation between the virtual cameras is necessary. The disadvantage of this system is that one virtual camera consists of only one fourth of the active image format. The slightly reduced accuracy caused by the mirror system is pointed out in [6].

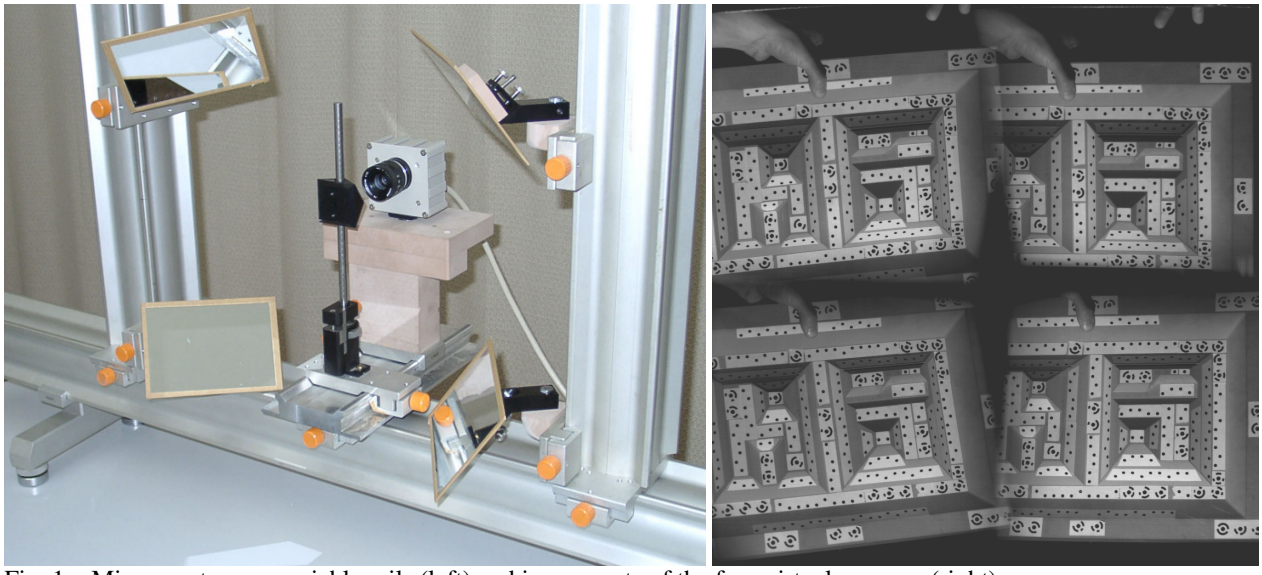

Fig. 1 – Mirror system on variable rails (left) and image parts of the four virtual cameras (right)

The used tracer particles for experiments in this draw channel are small Styrofoam spheres with diameters of 0.1 or 0.5 mm. Although they do not have perfect flow following capability they are easy to handle and to analyse. An approach to adjust the 3D trajectories affected by the tracer characteristics is shown in [1]. The observation volume is illuminated by the fuzzy focal points of halogen spot lights with fresnell lenses [5].

2.2 Experiment B – ILKA

Another application for the developed algorithms of 3D PTV is the large scale convection in huge cells (ILKA and Ilmenauer Fass) [8]. The cell ILKA is 3 x 3 x 4 m³ with the cameras and illumination inside. Caused by the dimension of the observation volume four SRL cameras with an image resolution of 8 MPixel are mounted in four corners of one boundary. This affords to detect the tracer – in this case helium filled soap bubbles [2][8] – with diameters of less than 1 cm. Currently halogen spot lights are used for the illumination. Because of the thermic sensibility of the cell other illumination techniques have to be installed to avoid thermic input.
Due to the large depth range the tracer particles occur very densely in the images. Hence to solve the multi image matching a high accuracy is necessary although the application's main focus is turned to large trajectories which represent the convection structures.

3 ANALYSIS CHAIN

The following chapter introduces the workflow of 3-D PTV. The flow chart shown in figure 2, points out necessary steps of the workflow that is utilised in order to get 3D trajectories. The workflow can be divided into three main parts: image processing, determination of object coordinates (spatial matching) and tracking (temporal matching). The system calibration contains the determination of the orientation and the characteristics of the cameras in a prior step. The single worl steps are independent on each other. The observation volume and the velocity do not influence the analysis.

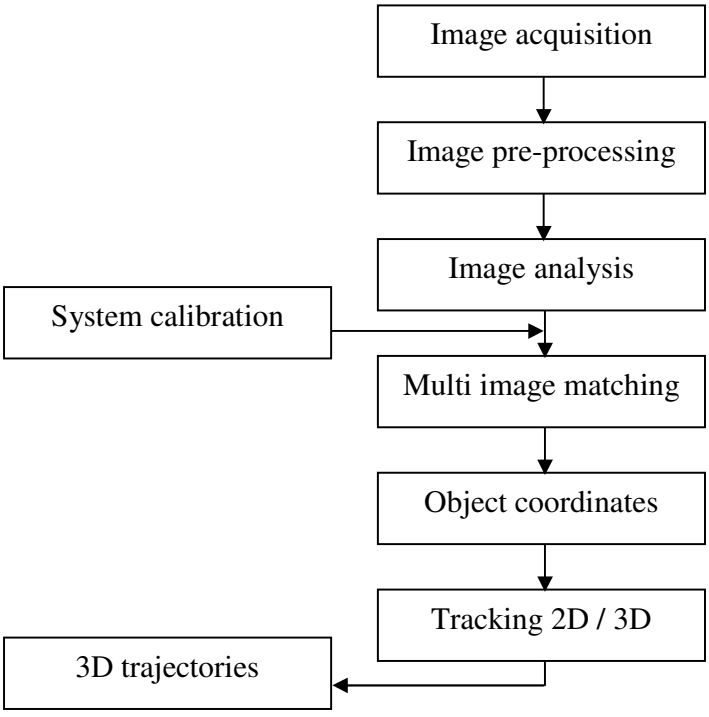

Fig. 2 – Workflow

3.1 Image processing

In order to extract image coordinates with sub-pixel precision, the following steps are applied to the image sequences: First a background image is created by a temporal histogram analysis. This is subtracted from all original images. In the created difference images, discrete tracer particles are segmented by a region growing approach supported using a discontinuous criterion [4]. This has to be done to divide overlapping tracer particles. Applying a centroid algorithm, the image coordinates are determined with sub-pixel precision. The centroid of an object blurred by velocity is close to the average position during the exposure time [10]. Consequently, the blurring does not influence the image coordinates significantly (in case of linear movement). Furthermore the blurring includes information about the motion direction of each tracer particle. This can be used as additional knowledge for the temporal matching.

3.2 Object coordinate determination

The 3D object coordinates are calculated from the image coordinates of homologous image points. Therefore, it is necessary to link all related image points representing one tracer in the object space. This matching is supported using the epipolar constraint and approximate depth information about the point cloud. In case of using only two images, all image points within a certain distance to the epipolar line are candidates, thus ambiguities cannot be solved in a densely packed flow. A third camera reduces the search space for corresponding particles from a line (plus tolerance) to the intersection points of lines (Figure 3)[3]. It can be shown that the use of a third camera reduces the probability of occurrence of ambiguities by the factor 10...100. For most applications an unambiguous solution is possible. This requires that the orientation parameters are well determined and every tracer particle is represented in each image. If this is not the case, ambiguities cannot be solved or tracer positions get lost.

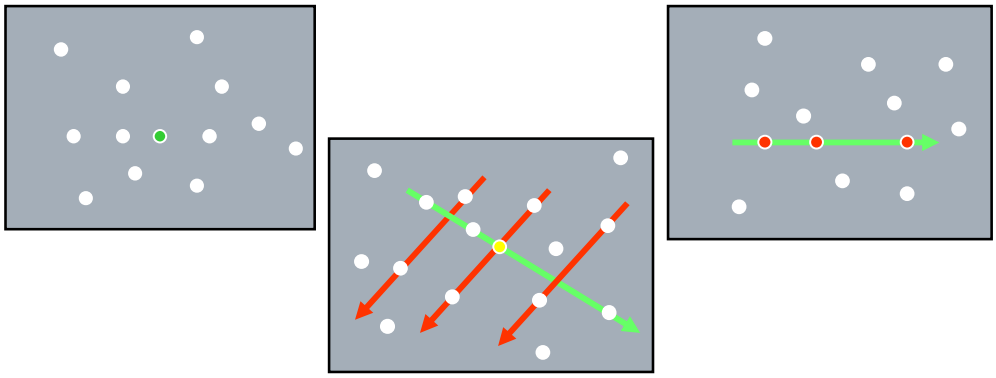

Fig. 3 – Solving multi image matching using epipolar lines in 3 images (following [4])

90% of the remaining ambiguities can be solved using a fourth camera. This provides much more information. Hence, weaker camera orientations or hidden particles in an image can also be successfully analysed. Because of the higher amount of information, other ambiguities have to be solved. Using image point triples, the image point in the fourth image can be calculated. If there is no candidate in the search area, there are two possibilities: The tracer can be hidden or the candidates of the image point triple are no homologous image points. Whether the object point is calculated with three of four image points or not, is decided by a probability based algorithm.

3.3 Spatial matching

After image processing to determine the object coordinates of all epochs, lots of unconnected point clouds are available. At that time they do not include any information about the velocity field. There are different approaches to calculate this information. They can be global or local in two or three dimensional data sets [9]. The used tracking algorithm is local and spatial based. This means that for each object coordinate triple (each tracer and each epoch) a position in the following epoch is predict. Using decision rules and connectivity analysis long trajectories with 5 to 80 nodes (maximum depends on the residence time in the observation area) can be generated.
Using the tracking in image space additionally the redundancies of multi image matching and tracking can be used for a loop check. As shown in [1] it will be necessary to correct the tracer path because of their drift. This means that the original trajectories do not represent the flow field but for each node a corrected velocity vector can be determined.

4 RESULTS

As one can see in the analysis chain different results are available. There are object coordinates of all tracers at all epochs. All of these unique coordinate triples belong to the same accuracy level and are not correlated (except the orientation parameters). The accuracy potential depends on the image point measurement, the system orientation and the object size respectively the distance between camera and target.
These independent 3D positions lead to positive effects of the trajectory accuracy. One trajectory consists of two nodes. It is obvious that the length of the vector (distance between two nodes) influences its accuracy concerning the length and the direction. Figure 4 shows this effect and reason that long single trajectories (distance between two nodes) consist of a higher relative accuracy. Long connected trajectories (lots of nodes) can be smoothed to improve the single node accuracy.

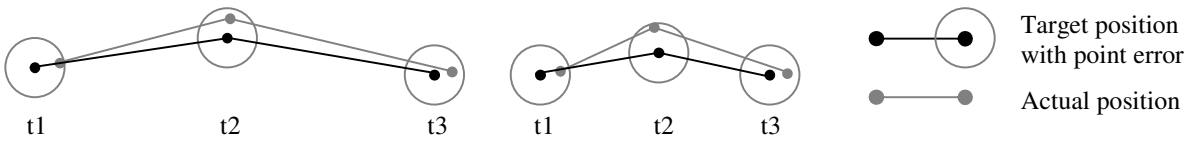

Fig. 4 – Influence of point error on length and direction of trajectories

The used tracking algorithm has to consider the ration between 3D object coordinate accuracy and trajectory length. A correct prediction to the succeeding epoch depends on the true direction (in case of long trajectories) or the true length (in case of short trajectories). Using error propagation (equation (1)) of 3D point error ($\sigma_{Pt1}/\sigma_{Pt2}$) it is possible to determine the error of the prediction for the spatial matching and to adapt the matching parameters.

$$\sigma_{P_{t3}}{}^2 = \left(\frac{\partial P_{t3}}{\partial l}\cdot\sigma_l\right)^2 + \left(\frac{\partial P_{t3}}{\partial r}\cdot\sigma_r\right)^2 + \left(\frac{\partial P_{t3}}{\partial P_{t2}}\cdot\sigma_{P_{t2}}\right)^2 \qquad (1)$$

$$\sigma_l^2 = \left(\frac{\partial l}{\partial P_{t1}} \cdot \sigma_{P_{t1}} \right)^2 + \left(\frac{\partial l}{\partial P_{t2}} \cdot \sigma_{P_{t2}} \right)^2 \quad (2)$$

$$\sigma_r^2 = \left(\frac{\partial r}{\partial P_{t1}} \cdot \sigma_{P_{t1}} \right)^2 + \left(\frac{\partial r}{\partial P_{t2}} \cdot \sigma_{P_{t2}} \right)^2 \quad (3)$$

The absolute accuracy does not depend on the size of the observation volume, the flow velocity or the used frame rate. In contrast the relative accuracy is higher with growing flow velocity and longer trajectories. But it is obvious that in this case the pre processing is more difficult [5].

4.1 Object coordinates

There are two different experiments called *A* (draw wind tunnel) and *B* (ILKA cell). Their configuration parameters are shown in table 1.

Characteristic	Experiment *A1* / *A2* (draw channel)	Experiment *B* (ILKA cell)
Size	40 x 40 x 40 cm³	4 x 3 x 4 m³
Tracer particles	Styrophoam 0.1 – 0.5 mm	Helium filled soap bubbles 1 cm
Camera system	High-speed camera-mirror system	4 SRL cameras
Pixel number and size	1 MPx - 12µm	8 MPx - 6.42 µm
Mean distance camera - tracer	1.5 m / 0.9 m	3 m
Mean base length	0.45 m	2.10 m
Base-depth ratio	1 : 3.3 / 1 : 2	1 : 1.4

Tab. 1 – Parameters of the experiments

The results can be evaluated using the standard deviations of each calculation step. At first the calibration target field with dot and code marks is determined with high accuracy. The standard deviations of these 3D points are shown in table 2.

	Experiment *A*	Experiment *B*
Size	30 x 50 x 5 cm³ - calibration board	3 x 3 x 1 m³ - cell boundary
Point number	289	91
Standard deviation – lateral	3 µm	0.10 mm
Standard deviation – depth	6 µm	0.15 mm

Tab. 2 – Properties of calibration fields

The orientation parameters of all cameras are determined within a resection. The resulting standard deviation of unit weight represents the accuracy potential of the used configuration (table 3). To demonstrate the potential, standard deviations are translated to point errors in the mean observation volume. Tapping the full potential requires same conditions as at the calibration. The image point measurement accuracy of 1/50 Pixel (Px) for dot marks using ellipsoid operator can not be achieved. Caused by shape and size of the tracer particles the centroid algorithm with a less sub-pixel accuracy

is necessary. Furthermore, using a mirror system in experiment *A* reduces the accuracy potential by factor 2-3 [6].

	Experiment *A1*	Experiment *A2*	Experiment *B*
σ_0	1.4 µm ≈ 1/9 Px	1.4 µm ≈ 1/9 Px	0.4 µm ≈ 1/15 Px
Lateral point error in mean distance	0.08 mm	0.05 mm	0.09 mm
Depth point error in mean distance	0.28 mm	0.10 mm	0.12 mm

Tab. 3 – Accuracy potential

The analysis of experiments using intersection yields 3D object coordinates with related standard deviations (table 4). Processing thousands of epochs with hundreds of tracers the determined accuracies show reliable values for the used measurement system. Different orders of magnitude in accuracy are caused by the different configurations and used cameras.

	Experiment *A1*	Experiment *A2*	Experiment *B*
σ_X	0.15 mm	0.07 mm	0.6 mm
σ_Y	0.15 mm	0.06 mm	0.6 mm
σ_Z	0.50 mm	0.12 mm	1.0 mm

Tab. 4 – Standard deviation of 3D object coordinates of tracer particles

Using more hardware effort in experiment *A* – especially more cameras with higher resolution – the accuracy will be enhanced by factor 3. Aim of experiment *B* is to analyse large scale structures. There it is not to achieve high single point accuracy but determine large connected trajectories. The resulting trajectories depending on the one hand on the 3D point accuracy but also on the length of vectors and trajectories.

4.2 Trajectories

Basic elements of a trajectory are vectors of one tracer in successive epochs. Quality criteria are cumulative length over all epochs and accuracy of each partial vector. The length and direction error of vectors caused by 3D point error of the nodes can be calculated with equations (2) and (3). The maximum number of a trajectory is limited by the residence time in the observation volume. It is also constrict by the number of epochs taken with the measurement system. Mostly the memory writing rate of cameras is the limiting fact.
Figure 5 shows some representative trajectories of both experiments *A* and *B*. One example of experiment *A* consists of 1000 epochs within 2 seconds. The longest trajectory contains 61 vectors. All trajectories in figure 5 left are longer than 20 epochs. The mean vector length averages 12 mm. Table 5 gives an overview about the length of the 3787 determined trajectories.

# vectors	≥ 30	≥ 25	≥ 20	≥ 15	≥ 10	10 to 4
# trajectories	5	4	75	749	1022	1932

Tab. 5 – Number and length of trajectories

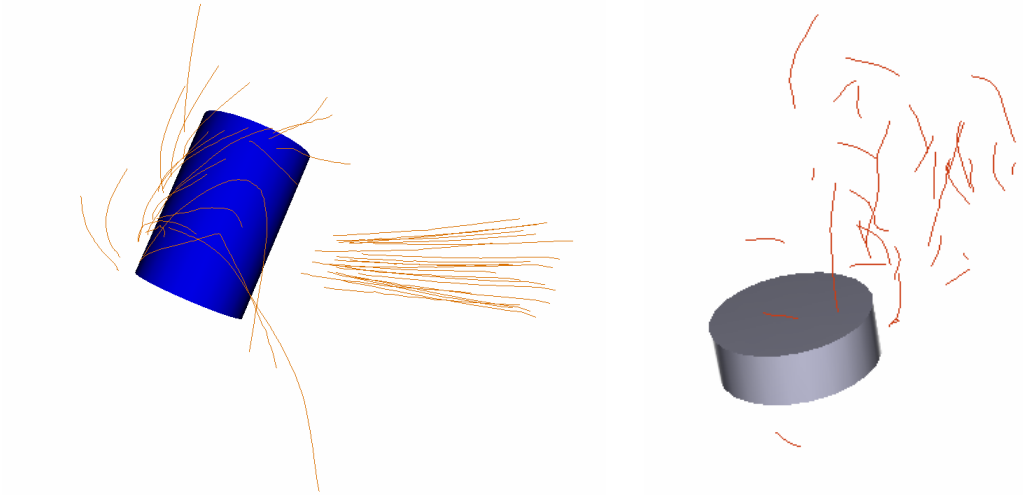

Fig. 5 – Trajectories behind a cylinder (left – experiment *A*), trajectories over a ventilator (right – experiment *B*)

An example of experiment *B* contains 20 epochs caused by the storage capacity of the used SLR cameras. Table 6 shows the distribution of the trajectory lengths. The mean vector length averages 30 mm. The system was triggered manual so velocities can not be calculated.

# vectors	≥ 15	≥ 10	≥ 5
# trajectories	6	5	36

Tab. 6 – Number and length of trajectories

4.3 Further analysis

The determined trajectories describe the path of each particle. Caused by the properties of the tracer, each velocity vector within a trajectory has to be corrected as shown in [1]. This leads to a not connected trajectory but gives at a current position and time a 3C velocity vector. For further analysis an interpolation to a regular grid can be processed.
To verify the system some experiments with defined motions and comparable experiments to established flow measurement systems will be carried out.

5 CONCLUTION

In this article we present the 3D Particle Tracking Velocimetry (3D PTV) measurement system and its potential for flow field determination. It affords to determine a time resolved 3D3C flow field while either hundreds of epochs or some seconds. Modifying the hardware configuration several large observation volumes (up to some cubic metres) can be analysed.
The accuracy depends on a lot of parameters. It is shown that a 3D point error of less than 1/10 mm in smaller and 1 mm in large volumes can be achieved. The accuracy of trajectories depends on their lengths and on 3D point errors of their nodes.

6 ACKNOLEDGEMENT

The work presented in this paper was supported by “Deutsche Forschungsgesellschaft” (DFG) within the SPP 1147. The author’s gratitude also goes to Dr. K. Hoyer (IHW, ETH Zurich) for producing hardware components of the mirror system and to the “Institut für Luft- und Raumfahrttechnik” for supporting my experiments.

REFERENCES

1. Frey J, Putze T and Grundmann R. Räumliches PTV in Gasströmungen und Ansätze zur Korrektur des begrenzten Partikelfolgevermögens. *Proceedings der 14. GALA-Fachtagung "Lasermethoden in der Strömungsmeßtechnik”*, Braunschweig, 2006.
2. Machacek M and Rösgen T. A Quantitative Visualization Method for Wind Tunnel Experiments Based on 3D Particle Tracking Velocimetry (3D-PTV). *PAMM, Proc. Appl. Math. Mech. 1*, 2002.
3. Maas H-G. Complexity analysis for the determination of image correspondences in dense spatial target fields. *International Archives of Photogrammetry and Remote Sensing*, Vol. 29, Part B5, pp 102-107, 1992.
4. Maas H-G, Grün A and Papantoniou D. Particle tracking in threedimensional turbulent flows. Part I: Photogrammetric determination of particle coordinates. *Experiments in Fluids*, Vol. 15, pp 133-146, 1993.
5. Putze T. Einsatz einer Highspeedkamera zur Bestimmung von Geschwindigkeitsfeldern in Gasströmungen. *24. wissenschaftlich- technische Jahrestagung der DGPF*, pp 325 – 332, 2004.
6. Putze T. Geometric modelling and calibration of a virtual four-headed high speed camera-mirror system for 3-D motion analysis applications. *Optical 3-D measurement techniques VII*, pp 167 – 174, 2005.
7. Putze T and Hoyer K. Modellierung und Kalibrierung eines virtuellen Vier-Kamerasystems auf Basis eines verstellbaren Spiegelsystems. *Beiträge der Oldenburger 3D-Tage 2005*, Herbert Wichmann Verlag, Heidelberg, 2005.
8. Resagk C, Lobutova E, Rank R, Müller D, Putze T and Maas H-G. Measurement of large-scale flow structures in air using a novel 3D Particle Tracking Velocimetry technique. *13th Int. Symp on Appl. Laser Techniques to Fluid Mechanics*, Lisbon, Portugal, 2006.
9. Ruhnau P, Gütter C, Putze T, Nobach H and Schnörr C. A Variational Approach for Particle Tracking Velocimetry. *Measurement, Science & Technology 16*, pp 1449 – 1458, 2005.
10. Wierzimok D and Hering F. Quantitative Imaging of Transport in Fluids with Digital Image Processing. *Imaging in Transport Processes*, Begell House, pp 297-308, 1993.